Experimental Induction and Three-Dimensional Two-Photon Imaging of Conjunctiva-Associated Lymphoid Tissue

Philipp Steven,[1,2] *Jan Rupp,*[3] *Gereon Hüttmann,*[4] *Norbert Koop,*[4] *Carmen Lensing,*[3] *Horst Laqua,*[1] *and Andreas Gebert*[2]

Purpose. Conjunctiva-associated lymphoid tissue (CALT) is assumed to be a key location for the generation of adaptive immune mechanisms of the ocular surface, but functional studies of CALT are still lacking. The purpose of this study was to establish an animal model that enables functional analysis of immune mechanisms going on within CALT. In addition, the use of two-photon microscopy, a new optical method, was evaluated for examining complex immunologic interactions of CALT by volume (three-dimensional [3-D]) and time-dependence (four-dimensional [4-D]) in vivo.

Methods. The conjunctiva of female BALB/c mice was repeatedly challenged with topical *Chlamydia trachomatis* serovar C or a solution of ovalbumin and cholera toxin B. Two-photon microscopy was conducted on explanted, unfixed, and unstained eyes with adjacent nictitating membranes.

Results. After three to five stimulations, CALT was detected exclusively in the nictitating membrane of 73% (*C. trachomatis*) or 70% (ovalbumin/ cholera toxin) of the animals. CALT mainly consisted of CD45R/B220$^+$ B cells and CD4$^+$ and CD8$^+$ T cells. Electron microscopy showed intraepithelial lymphocytes and follicles consisting of lymphocytes, dendritic cells, and macrophages. Two-photon microscopy based on tissue autofluorescence allowed all components of CALT to be detected three dimensionally. High-resolution images were generated in tissue depths of 65 μm below the mucosal surface.

Conclusions. This study introduces a novel mouse model for functional investigations of CALT. Topical stimulation with *C. trachomatis* or ovalbumin/cholera toxin B reliably leads to CALT generation at the nictitating membrane. The use of two-photon microscopy enables groundbreaking 3-D and, in the future, intravital 4-D investigations of immunologic processes initiated in CALT. (*Invest Ophthalmol Vis Sci.* 2008;49: 1512–1517) DOI:10.1167/iovs.07-0809

Microbial and nonmicrobial pathogens constantly challenge the human organism. An effective defense system is needed, to maintain mucosal integrity and to prevent pathogen invasion. Besides the innate immune system, with antimicrobial peptides, mucins, macrophages, and neutrophils,[1] the adaptive immune system plays the key role in host defense. Mucosa-associated lymphoid tissue (MALT) is present in many mucosal sites,[2] administering the adaptive immune mechanisms of antigen uptake, antigen processing, lymphocyte activation, and consecutive immunoglobulin secretion or T-cell effector functions.[3] Whereas morphology and function of MALT locations like Peyer's patches, tonsils, appendix, and bronchus-associated lymphoid tissue (BALT) are well characterized, there has been no detailed analysis of the conjunctiva-associated lymphoid tissue (CALT). This deficit in information is surprising, because adaptive immune mechanisms of the conjunctiva are critically involved in diseases such as Sjögren's and dry eye syndromes; conjunctival allergy; various forms of bacterial, viral, and parasitic conjunctivitis, and corneal transplant rejection.[4–10]

To investigate the function of CALT and its involvement in immunologic processes, an animal model is needed that allows intravital investigations. Investigations of CALT that have been performed in other species (e.g., guinea pig,[11] rabbit,[12] dog,[13] and turkey,[11,14]) suffer from technical restrictions, such as, limited range and definition of immunologic tools, whereas to study the mouse, the preferred animal model in immunologic research, numerous techniques are available.

Comparative anatomic studies did not find CALT in laboratory mice.[15,16] In contrast, observations by Sakimoto et al.[17] show that the nictitating membrane (plica semilunaris), a rudimentary residue of a third eyelid, contains organized lymphoid tissue, and recently, Astley et al.[18] investigated New World rodents, with similar findings, all of which demonstrates that the mouse represents a suitable model for investigating CALT and its functional relation to immune mechanisms of the ocular surface. As CALT is rarely present in unstimulated laboratory mice (own observations), we applied a stimulus to increase CALT expression. In the present study, we used *Chlamydia trachomatis* serovar C or a solution of ovalbumin and cholera toxin B (OVA/CT-B) as stimuli. *C. trachomatis* was chosen, as this microbial pathogen induces a follicular conjunctivitis in humans, and BALB/c mice are known to be susceptible to *C. trachomatis* infections.[19] OVA/CT-B was chosen to apply a nonmicrobial pathogen that is commonly used and well defined in studies of mucosa immunology.[20,21] A mouse model further allows immune mechanisms within CALT to be directly visualized by microscopy. As the conjunctiva is easily accessible, the application of high-resolution imaging techniques could even enable the analysis in vivo. Two-photon microscopy is a promising imaging technique for such intravital investigations of immune mechanisms,[22] since it generates three-dimensional image stacks by exciting tissue autofluorescence without relevant cellular photodamage or photobleaching.

The purpose of this investigation was to establish a mouse model that reliably expresses CALT for functional analysis by autofluorescence two-photon microscopy.

From the [1]Eye-Hospital, the [2]Institute of Anatomy, the [3]Institute of Medical Microbiology and Hygiene, and the [4]Institute of Biomedical Optics, University of Lübeck, Lübeck, Germany.

Supported by the Medical Faculty, University of Lübeck, Grant No. A02-2006.

Submitted for publication July 2, 2007; revised September 12 and December 3, 2007; accepted February 20, 2008.

Disclosure: **P. Steven**, None; **J. Rupp**, None; **G. Hüttmann**, None; **N. Koop**, None; **C. Lensing**, None; **H. Laqua**, None; **A. Gebert**, None

The publication costs of this article were defrayed in part by page charge payment. This article must therefore be marked "*advertisement*" in accordance with 18 U.S.C. §1734 solely to indicate this fact.

Corresponding author: Philipp Steven, MD, Eye Hospital and Institute of Anatomy, University of Luebeck, Ratzeburger Allee 160, 23538 Luebeck, Germany; psteven@gmx.de.

METHODS

Fifty female BALB/c mice, 12 weeks of age, were obtained from Charles River Laboratories (Sulzfeld, Germany). Care and treatment of the animals were undertaken in accordance with the regulations of the University of Lübeck and the ARVO Statement for the Use of Animals in Ophthalmic and Visual Research. All treatments were performed with the mice under deep anesthesia with ketamine (Ketanest S; Pfizer, Freiburg, Germany) and xylazine (Rompun vet; Bayer Health Care, Berlin, Germany).

Topical Conjunctival Stimulation with *C. trachomatis* or OVA/CT-B

Stocks of *Chlamydia trachomatis* (serovar C) were grown on HeLa cells, according to a standard protocol.[23] Elementary bodies were harvested, centrifuged, and diluted with sucrose-phosphate-glutamic acid buffer (SPG). Five microliters containing 5000 IFU *C. trachomatis* were applied topically to each eye of 24 mice with a sterile pipette on day 0, 2, 4, 6, and 8. Twelve female mice received a nontraumatic inoculation of 5 μL of a mixed solution of 0.25 μg/mL ovalbumin (OVA) and 0.1 μg/mL cholera toxin B (CT-B) on days 0, 2, and 4. As a control, six animals received 5 μL SPG topically on days 0, 2, 4, 6, and 8. On days 5, 7, 9, 11, 13, and 15, seven animals (four animals/eight eyes, *C. trachomatis* stimulated; two animals/four eyes, OVA/CT-B stimulated; and one animal/two eyes, SPG control) were euthanized, and the eyes with adjacent conjunctiva were dissected (Table 1).

Immunohistochemistry and Transmission Electron Microscopy

The dissected ocular tissue was either frozen in liquid nitrogen for immunohistochemistry (IHC) or fixed in a solution containing 2% glutaraldehyde and 0.6% paraformaldehyde in 0.1 M Na-cacodylate buffer for transmission electron microscopy (TEM). The specimens were embedded in Araldite (Merck, Darmstadt, Germany), and semi- and ultrathin sections were prepared and examined by light and electron microscopy (Axioskop 2; Carl Zeiss Meditec, Oberkochen, Germany; and EM 400 T; Philips, Eindhoven, The Netherlands). Frozen specimens were serial sectioned with a cryostat and stained with toluidine blue. Immunohistochemical analysis was conducted with anti-mouse antibodies directed against CD45R/B220, CD4, follicular dendritic cells (FDCs; BD Pharmingen, San Diego, CA), and CD8 (Santa Cruz Biotechnologies, Santa Cruz, CA). Alexa Fluor 488 or 555 goat-anti-rat antibodies (Invitrogen, Carlsbad, CA) or a biotinylated rabbit-anti-rat antibody (Dako, Glostrup, Denmark) were used as secondary antibodies to reveal labeled cells. Nuclear counterstaining was conducted with Hoechst 33258 (Sigma-Aldrich, St. Louis, MO).

Two-Photon Microscopy

The two-photon microscope (Dermainspect; Jenlab, Jena, Germany) was equipped with a tunable infrared femtosecond-laser (720–920 nm tuning range; Wide Band MaiTai; Spectra Physics, Mountain View, CA). After the animals were euthanized, the eyes, together with adjacent conjunctiva were removed and immediately glued into a six-well plate using Vetbond (3M, St. Paul, MN). Without further fixation, the specimens were covered with DMEM/F12 (Invitrogen) and examined (IR Achroplan LD 40/0.80 W objective; Carl Zeiss Meditec). Autofluorescence image stacks of CALT regions were made at 730 nm excitation wavelength and comprised up to 80 images and volumes up to 200 × 200 × 70 μm.

RESULTS

Histologic Analysis of Induced CALT

Topical application of *C. trachomatis* or OVA/CT-B reliably induced lymphocyte aggregates in the conjunctiva of the nictitating membrane (Fig. 1, Table 1). Overall expression rates of 73% CALT in *C. trachomatis*-stimulated and 70% in OVA/CT-B-stimulated animals were obtained. The highest expression rates were from day 8 to 11 after first stimulation. Control specimens revealed no organized lymphoid tissue, except one animal on day 9 that showed one small lymphoid aggregate.

Conventional histology and TEM showed lymphoid aggregates of varying shape and size located beneath the outer surface of the nictitating membrane (Fig. 2). The covering stratified squamous epithelium was thinned, presenting only two to four cell layers and containing numerous lymphocytes within intraepithelial pockets (Fig. 3). In this lymphoepithelium, goblet cells were absent, whereas they were evenly distributed in the remaining epithelium of the nictitating membrane (data not shown). The spaces between lymphoepithelium and lymphoid aggregates contained few lymphocytes located within loose connective tissue. The aggregates were mainly composed of closely arranged lymphocytes, cells that have dendritic cytoplasmic protrusions and macrophages (Fig. 3). Blood and lymphatic vessels were located in close relation to or within the aggregates. Lymphatic capillaries possessed a thin endothelium with overlapping cellular processes and displayed a large lumen relative to the thickness of the wall in comparison to blood capillaries. The blood capillaries were fed by two prominent vessels that emerged from the adjacent tarsal conjunctiva and extended along either margin to the apex of the nictitating membrane. Certain blood vessels showed a thickened endothelium with cytoplasmic extensions that protruded toward the lumen. Intravascular lymphocytes were preferentially located at the aggregate-facing side of the blood vessels, migrating across the vessel wall (Fig. 2c). IHC showed that the lymphoid aggregates contained lymphocyte subsets, typical for primary lymphoid follicles. The center of these follicles was predominantly composed of CD45R/B220$^+$ B cells (Fig. 2). A few CD8$^+$ and CD4$^+$ T cells (Fig. 2) were located within the center but mainly surrounding the B cells,

TABLE 1. Stimulation Protocol and CALT Expression

	C. trachomatis (n = 48 eyes)		OVA/CT-B (n = 24 eyes)		Control (n = 12 eyes)		
Day	**Stimulation**	**CALT/Eyes**	**Stimulation**	**CALT/Eyes**	**PBS**	**CALT/Eyes**	**Dissection**
0	+		+	−	+		
2	+		+		+		
4	+		+		+		
5		4/8		2/4		0/2	+
6	+	−			+		
7		4/8		3/4		0/2	+
8	+				+		
9		8/8		3/4		1/2	+
11		7/8		4/4		0/2	+
13		6/8		3/4		0/2	+
15		6/8		2/4		0/2	+

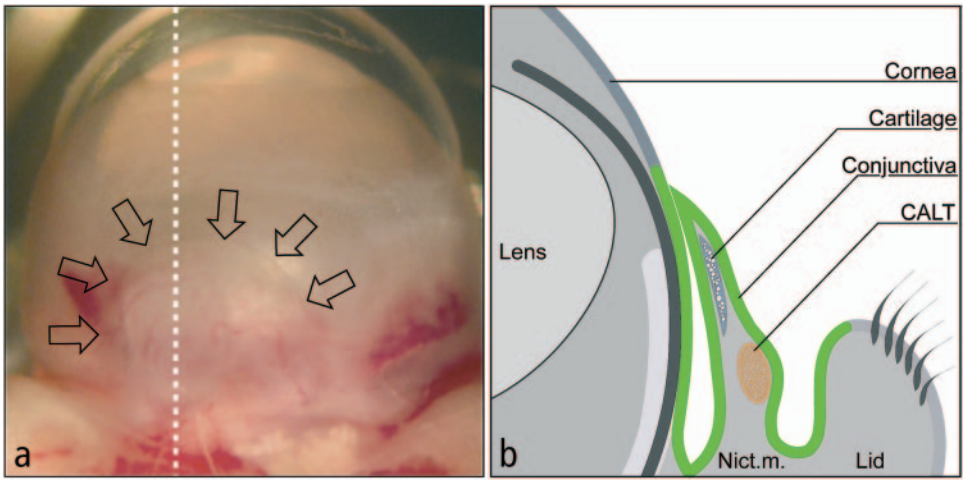

FIGURE 1. (**a**) Explanted eye with adjacent nictitating membrane (*arrows*). *Dotted line*: section plane seen in (**b**). (**b**) Diagram of the structural relation between nictitating membrane, CALT, and eyeball. The bulbar conjunctiva extends seamlessly toward the nictitating membrane to the tarsal conjunctiva. CALT is located on the outward-facing side of the membrane. Nict. m., nictitating membrane.

whereas a few $CD8^+$ T cells were detected within the epithelium. Follicular dendritic cells were not detected by IHC.

No morphologic differences or differences in the composition of lymphocyte subsets were noted between *C. trachomatis* and OVA/CT-B-induced aggregates. *C. trachomatis*-stimulated animals did not show any signs of destruction of the conjunctiva. Apart from the follicles generated, the mucosa of the stimulated animals did not differ from that of the control animals and showed no accumulation of inflammatory cells.

Two-Photon Microscopy of CALT

Two-photon microscopy of fresh, unfixed conjunctival tissue produced high-contrast autofluorescence images of the lymphoid follicles. The nonlinear effect of two-photon excitation resulted in a strong signal and low noise by producing autofluorescence in a small focal volume as a precondition for the generation of high-resolution images in scattering tissues (Fig. 4). Pictures that featured a resolution better than 1.0 μm were made at depths of 65 μm or more. At a 730-nm excitation wavelength, sections parallel or perpendicular to the surface revealed epithelial cells with bright cytoplasm and dark nuclei. Superficial, intermediate, and basal cell layers of the epithelium could be distinguished by the reduction of cell size and shape (Figs. 4b, 4c). The transition between basal epithelial cell layers and subepithelial lymphocytes was clearly demarcated by the nonfluorescing basal lamina (Fig. 4d). In the subepithelial tissue, fibroblasts, macrophages, and lymphocytes could be readily distinguished by their morphology and fluorescence intensity. According to light and electron microscopic observations, the lymphocytes showed a thin rim of cytoplasm surrounding their dark round nucleus, whereas fibroblasts were larger and possessed spindle-shaped processes of the cytoplasm. Macrophages displayed the highest intensity of autofluorescence with clearly detectable cytoplasmic inclusions (Fig. 4i). All cells were located within a network of bright fluorescing fibers of the connective tissue. Fifteen to 20 μm beneath the basal cell layer of the epithelium, lymphoid follicles extended downward, and individual lymphocytes could be identified at depths of 65 μm below the conjunctival surface (Figs. 4e, 4f). In close relation to the follicles, displaying clearly visible vessel walls, blood capillaries filled with erythrocytes (not shown) and lymphatic vessels containing typical endothelial folds (Figs. 4e, 4f) were located.

DISCUSSION

CALT has not yet been included in functional immunologic studies. Instead, based on merely morphologic studies, the

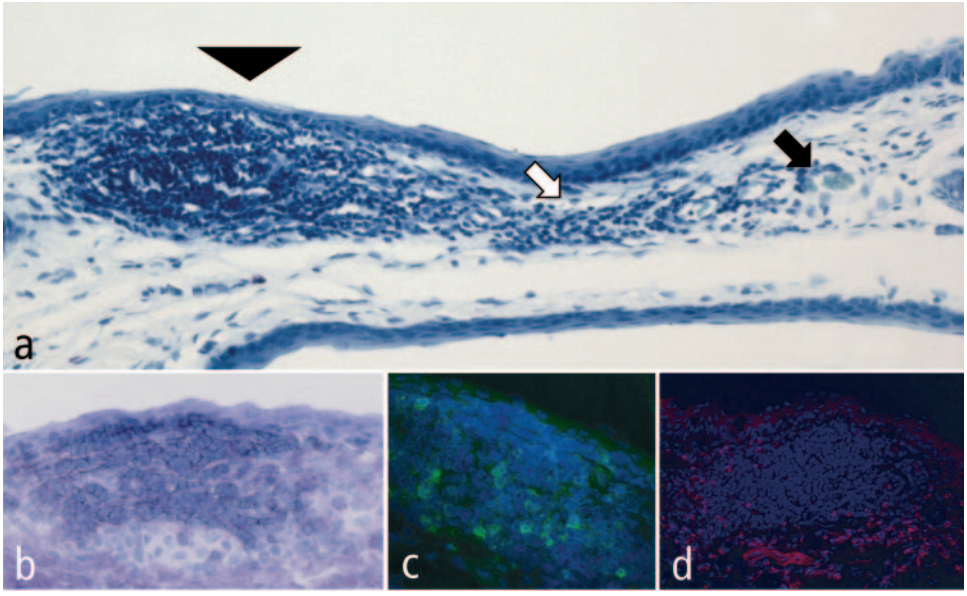

FIGURE 2. (**a**) Cross section through the nictitating membrane after *C. trachomatis* stimulation. A lymphoid follicle is located beneath the lymphoepithelium (*arrowhead*) in close relation to lymphatic vessels (*white arrow*) and blood capillaries (*black arrow*); (**b**) CD45R/B220+ B cells; (**c**) $CD8^+$ T cells; (**d**) $CD4^+$ T cells. Toluidine blue; magnification: (**a**, **d**) ×200; (**b**) ×320; (**c**) ×280.

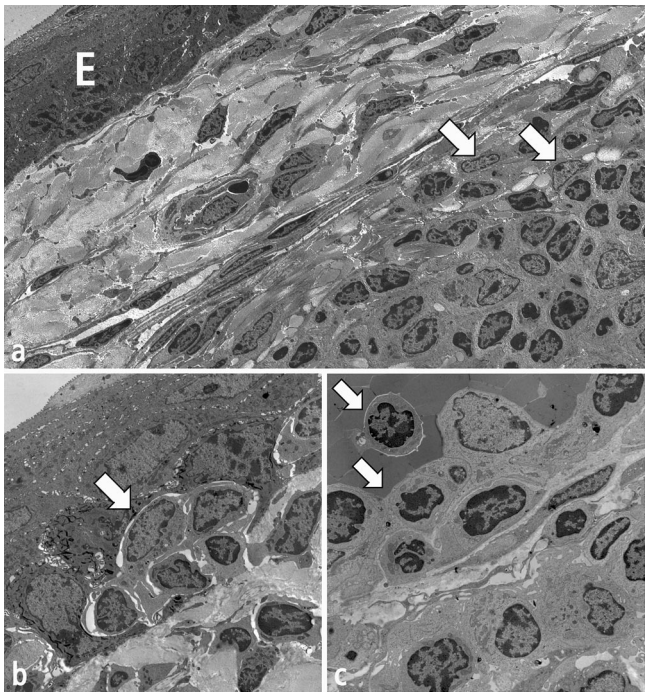

FIGURE 3. Electron microscopy of CALT. (**a**) A lymphoid follicle containing densely packed lymphocytes and dendritiform cells (*arrows*) is located below the epithelium (E) within the subepithelial space. (**b**) Lymphoepithelium: Lymphocytes (*arrow*) are located within epithelial pockets. (**c**) Intravascular lymphocytes penetrate the vessel wall (*arrows*) at the follicle-facing side. Magnification: (**a**) ×2100; (**b**) ×2900; (**c**) ×3200.

function of CALT has been derived from the well-established theory of MALT function.[24] In this context, it is concluded that B cells proliferate within CALT, recirculate and consecutively produce IgA in the conjunctiva and the lacrimal gland. It has even been hypothesized that CALT is involved in an immune privilege of the ocular surface.[25] The present study demonstrates that, under defined experimental conditions, mice generate organized lymphoid tissue in the nictitating membrane, with high reproducibility. This tissue consists of a lymphoepithelium, lymphoid follicles with B- and T-cell zones, adjacent blood vessels that have thickened endothelia as well as lymphoid vessels. As these components are characteristic for MALT, the term murine CALT is justified. In this context, we encounter the nictitating membrane as part of the conjunctiva (Fig. 1), for several reasons: (1) Both regions, nictitating membrane and the rest of the conjunctiva (bulbar and tarsal) are covered by the characteristic multilayered epithelium. (2) This epithelium seamlessly extends from the nictitating membrane toward the rest of the conjunctiva. (3) Nictitating membrane and conjunctiva share one network of blood vessels. These findings are in agreement with those in earlier reports,[26] and therefore a functional differentiation or compartmentalization seems not to be adequate.

FDCs were not found within the generated follicles, indicating that cells having ultrastructural features of dendritic cells could represent interdigitating dendritic cells (IDCs). The paucity of FDCs fits the findings in BALT in mice.[27] BALT has been investigated in detail[28] and contains lymphoid follicles bearing a B-cell zone and a T-cell zone that structurally resemble CALT. Although BALT is not present in the normal lung of adults, the functional relevance of BALT for the mucosal immune protection is generally accepted, and the term bronchus-associated lymphoid tissue is well established.

Earlier investigations did not report that CALT is present in the conjunctiva of unstimulated laboratory BALB/c mice,[15] and the authors did not report whether the nictitating membrane was included in the morphologic analysis. Our findings showed CALT exclusively on the outer surface of the murine nictitating membrane. We interpret the specific location of CALT as a consequence of a tear-film–dissolved pathogen accumulation before drainage through the efferent tear duct, whose openings are located opposite the nictitating membrane. Therefore, the duration of mucosa pathogen contact is likely to be the longest in this area, leading to the induction of CALT. In analogy, BALT is mostly located at bifurcations of the bronchi where airflow turbulences likewise might accumulate airborne pathogens.[28]

Topical conjunctival challenge with *C. trachomatis* (Serovar C) or ovalbumin with cholera toxin B reliably generated CALT in 70% (OVA/CT-B) or 73% (*C. trachomatis*) of the eyes investigated. Even though an invasion of chlamydiae could be demonstrated by immunohistochemical detection of intracellular inclusions (data not shown), the mice did not develop ocular surface destruction or further clinical signs of inflammation such as lid thickening or erythema. The frequency and extension of OVA/CT-B-induced CALT was similar to *C. trachomatis*-induced CALT and the cellular and structural components of CALT were comparable in both experiments. In the control group, CALT was present in only 1 (8%) of 12 eyes. The formation of lymphoid follicles within two weeks after initial stimulation is concordant with previous findings of Sakimoto et al.[17] The early conjunctival response stands in contrast to the 14-day latent period of systemic immune responses, but may be characteristic of the investigated nictitating membrane of the mouse.

Within CALT, CD45/B220$^+$ B cells and CD4$^+$ and CD8$^+$ T cells were found predominantly. Further studies should be focused on the functional relevance of better defined T- and B-cell subsets in the two types of stimulation. Whereas topical stimulation of the conjunctiva with ovalbumin is known to induce T-cell anergy,[29] chlamydia infection of the conjunctiva is associated with T- and B-cell activation.[30,31] Ocular surface diseases in humans exhibit a broad spectrum from most common conditions such as dry-eye syndrome and conjunctival allergy to less frequent but severe conditions, such as corneal transplant rejections, that often comprise difficulties in treatment. Our novel animal model allows various ocular surface diseases to be directly investigated in the near future with regard not only to CALT. Accepting the demonstrated requirement of previous pathogen stimulation, the continuing investigation of antigen-uptake and immunologic response related to CALT opens up fascinating perspectives.

We showed in the present study that two-photon microscopy has the potential to be a key technology in the study of antigen uptake, antigen processing, and immune reactions in the conjunctival compartment of living animals over hours. Without the use of intravital dyes, tissue preparations or transgenic animals (e.g., expressing green fluorescent protein variants) CALT and its overlaying epithelium is directly imaged at high resolution. All components of CALT lymphoepithelium, lymphoid follicle, and adjacent blood and lymphoid vessels can be visualized in three dimensions (3-D), and time lapse imaging of a certain tissue volume will achieve a 4-D analysis. In contrast to confocal microscopy, the investigation of highly scattering tissues such as lymphoid tissue is feasible in depths up to 90 μm with an unrivaled low risk of phototoxic damage. Assuming an ideal technical setup, a theoretical lateral resolution of 0.575 μm could be achieved that allows differentiating single mitochondria or lysosomes, for example. Besides fluorescence intensity, measurements of fluorescence-lifetime (FLIM) and spectral analysis of the excited fluorescence give

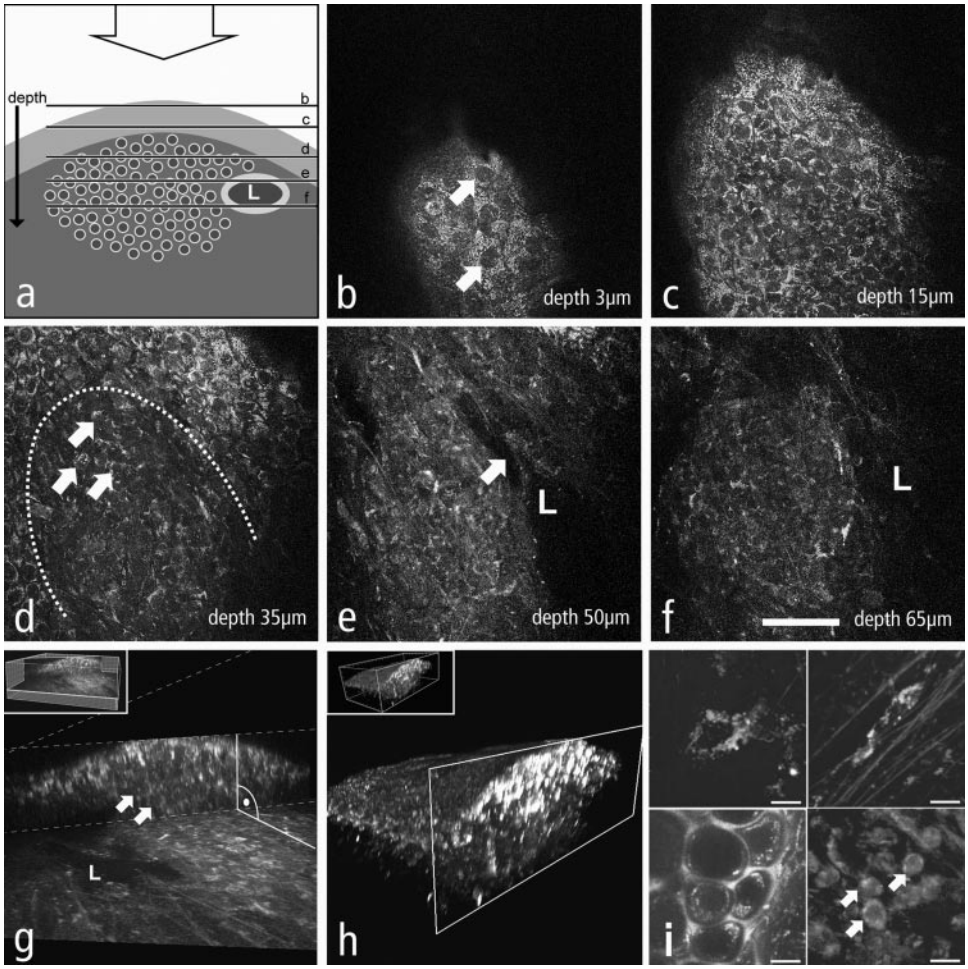

FIGURE 4. Two-photon microscopy of CALT. (**a**) Diagram of CALT with adjacent lymphatic vessel (L). *Large arrow*: orientation of the two-photon microscope objective. The section planes correspond to the images (**b**–**f**). (**b**) View parallel to the surface. Superficial epithelial cells had dark nuclei (*arrows*) and fluorescing cytoplasm. (**c**) Epithelial cell size decreased with scanning depth. (**d**) Subepithelial space with lymphocytes (*arrows*). *Dotted line*: transition between basal cell layer and subepithelial tissue. The lymphocytes, featuring a thin cytoplasmic rim, formed a lymphoid follicle. (**e**) A lymphatic vessel (L) with typical endothelial folds (*arrow*) was located in spatial relation to the follicle. (**f**) At a 65-μm depth, individual lymphocytes within the follicle were still distinguishable. Scale bar, 50 μm. (**g**) Three-dimensional reconstruction of the image stack. Two orthogonal section planes demonstrate epithelium, follicle and lymphatic vessel. Individual lymphocytes are distinguishable in the reconstruction (*arrows*). (**h**) Individual orientation of section planes allows extensive analysis of the 3-D structure of CALT. (**i**) High-resolution autofluorescence images of macrophages (*top left*), fibroblasts and connective tissue fibers (*top right*), lymphocytes (*arrows*, *bottom right*), and cartilage of the nictitating membrane (*bottom left*). Scale bar, 10 μm.

further functional information—for example, intracellular NAD(P)H metabolism[32]—and could lead to characteristic "fingerprints" of the different tissue components. Fluorescent microspheres or semiconductor nanoparticles (quantum dots) may be promising tools, because their highly defined emission spectra can easily be detected by means of spectral two-photon microscopy.[33] As described for lymph nodes, lymphocyte tracking will enable analyzing the immediate reaction of CALT by recording dynamic immunologic processes after experimental antigen exposure, such as accumulation of lymphocytes via blood vessels or antigen-directed migration.[34]

Taken together, our findings show two-photon microscopy to be a novel, powerful tool for performing functional intravital real-time studies of CALT in mice. It yields new options for investigating direct relationships between CALT and ocular surface diseases.

Acknowledgments

The authors thank Anke Hellberg and Claudia Kremling for excellent assistance preparing stimulants and specimens, Christo Örün for superb TEM-imaging and Judith Whittum-Hudson for helpful advice regarding chlamydia infections of mice.

References

1. Bals R. Epithelial antimicrobial peptides in host defense against infection. *Respir Res*. 2000;1:141–150.
2. Bienenstock J, Befus AD. Review: Mucosal immunology. *Immunology*. 1980;41:249.
3. Kraehenbuhl JP, Neutra MR. Molecular and cellular basis of immune protection of mucosal surfaces. *Physiol Rev*. 1992;72:853–879.
4. Rajagopalan G, Smart MK, Patel R, David CS. Acute systemic immune activation following conjunctival exposure to staphylococcal enterotoxin B. *Infect Immun*. 2006;74:6016–6019.
5. Fukushima A, Yamaguchi T, Ishida W, Fukata K, Ueno H. TLR2 agonist ameliorates murine experimental allergic conjunctivitis by inducing CD4 positive T-cell apoptosis rather than by affecting the Th1/Th2 balance. *Biochem Biophys Res Commun*. 2006;339:1048–1055.
6. Jones DT, Monroy D, Ji Z, Atherton SS, Pflugfelder SC. Sjögren's syndrome: cytokine and Epstein-Barr viral gene expression within the conjunctival epithelium. *Invest Ophthalmol Vis Sci*. 1994;35:3493–3504.
7. Pearlman E, Lass JH, Bardenstein DS, et al. Interleukin 4 and T helper type 2 cells are required for development of experimental onchocercal keratitis (river blindness). *J Exp Med*. 1995;182:931–940.
8. Niederkorn JY. Immunology and immunomodulation of corneal transplantation. *Int Rev Immunol*. 2002;21:173–196.
9. Micera A, Stampachiacchiere B, Aronni S, dos Santos MS, Lambiase A. Toll-like receptors and the eye. *Curr Opin Allergy Clin Immunol*. 2005;5:451–458.
10. Dua HS, Azuara-Blanco A. Corneal allograft rejection: risk factors, diagnosis, prevention, and treatment. *Indian J Ophthalmol*. 1999;47:3–9.
11. Latkovic S. The ultrastructure of the normal conjunctival epithelium of the guinea pig. III. The bulbar zone, the zone of the fornix and the supranodular zone. *Acta Ophthalmol* (*Copenh*). 1979;57:305–320.

12. Knop N, Knop E. Ultrastructural anatomy of CALT follicles in the rabbit reveals characteristics of M-cells, germinal centres and high endothelial venules. *J Anat*. 2005;207:409–426.
13. Giuliano EA, Moore CP, Phillips TE. Morphological evidence of M cells in healthy canine conjunctiva-associated lymphoid tissue. *Graefes Arch Clin Exp Ophthalmol*. 2002;240:220–226.
14. Fix AS, Arp LH. Conjunctiva-associated lymphoid tissue (CALT) in normal and Bordetella avium-infected turkeys. *Vet Pathol*. 1989; 26:222–230.
15. Chodosh J, Nordquist RE, Kennedy RC. Comparative anatomy of mammalian conjunctival lymphoid tissue: a putative mucosal immune site. *Dev Comp Immunol*. 1998;22:621–630.
16. McMaster PR, Aronson SB, Bedford MJ. Mechanisms of the host response in the eye. IV. The anterior eye in germ-free animals. *Arch Ophthalmol*. 1967;77:392–399.
17. Sakimoto T, Shoji J, Inada N, Saito K, Iwasaki Y, Sawa M. Histological study of conjunctiva-associated lymphoid tissue in mouse. *Jpn J Ophthalmol*. 2002;46:364–369.
18. Astley RA, Chodosh J, Caire W, Wilson GM. Conjunctival lymphoid follicles in new world rodents. *Anat Rec* (*Hoboken*). 2007;290: 1190–1194.
19. Whittum-Hudson JA, O'Brien TP, Prendergast RA. Murine model of ocular infection by a human biovar of Chlamydia trachomatis. *Invest Ophthalmol Vis Sci*. 1995;36:1976–1987.
20. Wikstrom ME, Batanero E, Smith M, et al. Influence of mucosal adjuvants on antigen passage and CD4+ T cell activation during the primary response to airborne allergen. *J Immunol*. 2006;177: 913–924.
21. Foss DL, Murtaugh MP. Mucosal immunogenicity and adjuvanticity of cholera toxin in swine. *Vaccine*. 1999;17:788–801.
22. Helmchen F, Denk W. Deep tissue two-photon microscopy. *Nat Methods*. 2005;2:932–940.
23. Siewert K, Rupp J, Klinger M, Solbach W, Gieffers J. Growth cycle-dependent pharmacodynamics of antichlamydial drugs. *Antimicrob Agents Chemother*. 2005;49:1852–1856.
24. Knop E, Knop N. Eye-associated lymphoid tissue (EALT) is continuously spread throughout the ocular surface from the lacrimal gland to the lacrimal drainage system (in German). *Ophthalmologe*. 2003;100:929–942.
25. Knop E, Knop N. The role of eye-associated lymphoid tissue in corneal immune protection. *J Anat*. 2005;206:271–285.
26. Setzer PY, Nichols BA, Dawson CR. Unusual structure of rat conjunctival epithelium: light and electron microscopy. *Invest Ophthalmol Vis Sci*. 1987;28:531–537.
27. Cesta MF. Normal structure, function, and histology of mucosa-associated lymphoid tissue. *Toxicol Pathol*. 2006;34:599–608.
28. Tschernig T, Pabst R. Bronchus-associated lymphoid tissue (BALT) is not present in the normal adult lung but in different diseases. *Pathobiology*. 2000;68:1–8.
29. Egan RM, Yorkey C, Black R, et al. In vivo behavior of peptide-specific T cells during mucosal tolerance induction: antigen introduced through the mucosa of the conjunctiva elicits prolonged antigen-specific T cell priming followed by anergy. *J Immunol*. 2000;164:4543–4550.
30. Perry LL, Feilzer K, Portis JL, Caldwell HD. Distinct homing pathways direct T lymphocytes to the genital and intestinal mucosae in Chlamydia-infected mice. *J Immunol*. 1998;160:2905–2914.
31. Pal S, Pu Z, Huneke RB, Taylor HR, Whittum-Hudson JA. Chlamydia-specific lymphocytes in conjunctiva during ocular infection: limiting dilution analysis. *Reg Immunol*. 1990;3:171–176.
32. Piston DW, Masters BR, Webb WW. Three-dimensionally resolved NAD(P)H cellular metabolic redox imaging of the in situ cornea with two-photon excitation laser scanning microscopy. *J Microsc*. 1995;178:20–27.
33. Stroh M, Zimmer JP, Duda DG, et al. Quantum dots spectrally distinguish multiple species within the tumor milieu in vivo. *Nat Med*. 2005;11:678–682.
34. Miller MJ, Wei SH, Cahalan MD, Parker I. Autonomous T cell trafficking examined in vivo with intravital two-photon microscopy. *Proc Natl Acad Sci USA*. 2003;100:2604–2609.